Electronic Supplementary Material (ESI) for ChemComm.
This journal is © The Royal Society of Chemistry 2016

# *SUPPORTING INFORMATION*

## Tetraphenylethene (TPE) modified polyhedral oligomeric silsesquioxanes (POSS): unadulterated monomer emission, aggregation-induced emission and nanostructural self-assembly modulated by the flexible spacer between POSS and TPE

Hui Zhou,[†] Jiesheng Li,[†] Ming Hui Chua,[†] Hong Yan,[†] Qun Ye,[†] Jing Song,[†] Ting Ting Lin,[†] Ben Zhong Tang*,[§] and Jianwei Xu*,[†,‡]

[†]Institute of Materials Research and Engineering, A*STAR (Agency for Science, Technology and Research), 3 Research Link, Singapore 117602, Republic of Singapore.

[‡]Department of Chemistry, National University of Singapore, 3 Science Drive 3, Singapore 117543, Republic of Singapore.

[§]Department of Chemistry, The Hong Kong University of Science & Technology, Clear Water Bay, Kowloon, Hong Kong, China.

*Corresponding author: Jianwei Xu
Email address: jw-xu@imre.a-star.edu.sg

Mailing address: 3 Research Link, Singapore 117602

Tel: 65-6872-7543

Fax: 65-6872-7528

# Table content

**Fig. S26** Illustration of self-assembly of TPE-modified POSS molecules in THF and THF/water. (*19*)

**Experimental**

**General.**

All synthetic manipulations were carried out under an atmosphere of dry argon gas using standard vacuum-line Schlenk techniques. All solvents were degassed and purified before use according to standard literature methods. Diethyl ether, hexanes, tetrahydrofuran, and toluene were purchased from Aldrich Chemical Co. Inc. and distilled from sodium/benzophenone ketyl before use.

**Instrumentation.**

$^{1}H$ and $^{13}C$ nuclear magnetic resonance (NMR) spectra were recorded on a Bruker DRX 400-MHz NMR spectrometer in $CDCl_3$ at room temperature using tetramethylsilane (TMS) as an internal standard. Operating frequencies of the NMR spectrometer were 400.13 MHz ($^{1}H$) and 100.61 MHz ($^{13}C$). MALDI-TOF was recorded using a Bruker Autoflex III TOF/ TOF. Elemental analysis was conducted on a Perkin-Elmer 240C elemental analyzer for C, H, and N determination. UV-vis and fluorescence spectra were obtained using a Shimadzu UV3101PC UV-vis-NIR spectrophotometer and a Perkin-Elmer LS 50B luminescence spectrometer with a Xenon lamp as light source, respectively. Thermal analysis was performed on a Perkin-Elmer thermogravimetric analyzer (TGA 7) in nitrogen or in air at a heating rate of 20 $^{o}$C/min and on a TA Instruments Differential Scanning Calorimetry (DSC) 2920 at a heating rate and a cooling rate of 5 $^{o}$C/min in nitrogen. Dynamic light scattering experiments were performed on a Brookhaven 90 plus spectrometer with a temperature controller. An argon ion laser operating at 633 nm was used as light source.

**General procedure for thiol-ene click reaction.**

A 5 mL schlenk flask was charged with compound **1** (445.8 mg, 0.5 mmol), Precursor-1 (307.4 mg, 0.5 mmol) and 1,4-Diazabicyclo[2.2.2]octane (DABCO, 5.6 mg, 0.005 mmol) was dried under reduced pressure at 60 $^{o}$C for 2 hours. It was then cooled to room temperature and anhydrous dimethyl sulfoxide/tetrahydrofuran (DMSO/THF, 2 mL, 1:1v/v), was introduced under argon atmosphere and purge for 15 mins. The reaction mixture was then heated to 60 $^{o}$C overnight with stirring, then mixture was cooled to room temperature and extracted with $CH_2Cl_2$ and washed with deionised water. The organic phase was isolated and dried over $MgSO_4$, followed by filtration and solvent was then removed under vacuum. The white crude product was purified via column chromatography on $SiO_2$ using $CH_2Cl_2$/hexane, 1:3 (v/v) as eluent to yield POSS-$AN_8$ as pale yellow gel-like solid.

**POSS-$AN_8$**. Yield: 61.2%; $^{1}H$ NMR ($CDCl_3$): $\delta$ 7.07-7.12 (m, 9H), 6.99-7.04 (8H, m), 6.84 (d, 2H, $J$ = 8.8 Hz), 2.76-2.87 (m, 4H), 2.57 (t, 2H, $J$ = 7.3 Hz), 1.79-1.91 (m, 7H), 1.70 (m, 2H), 0.95 (m, 42H), 0.69-0.74 (m, 2H), 0.60 (m, 14H). $^{13}C$ NMR ($CDCl_3$): $\delta$ 170.7, 132.7, 131.8, 131.7, 128. 2, 128.1, 128.0, 127.0, 126.9, 121.1, 35.5, 35.4, 30.1, 27.1, 26.1, 24.3, 24.2, 23.4, 22.8, 22.9, 12.0. $^{29}Si$ NMR ($CDCl_3$): $\delta$ -59.0. IR (thin film): $v$ = 3054, 3025, 2954, 2929, 2927,

2870, 1764, 1599, 1503, 1466, 1445, 1402, 1384, 1367, 1333, 1231, 1106, 954, 922, 867, 838, 802, 762, 746, 700 $cm^{-1}$. MALDI-TOF: [M] calcd for $C_{60}H_{92}O_{14}SSi_8$, m/z 1292.43; found, m/z 1292.31. Anal. Calcd for $C_{60}H_{92}O_{14}SSi_8$: C, 55.69; H, 7.17; S, 2.48; Si, 17.36. Found: C, 55.61; H, 7.29; S, 2.44; Si, 17.31.

**POSS-AN$_{15}$**. Yield: 58.4%; $^1$H NMR ($CDCl_3$): $\delta$ 6.99-7.14 (m, 15), 6.91 (d, 2H, *J* = 8.8 Hz), 6.62 (d, 2H, *J* = 8.9 Hz), 4.10 (t, 2H, *J* = 4.1 Hz), 3.87 (t, 2H, *J* = 6.5 Hz), 2.76 (t, 2H, *J* = 7.5 Hz), 2.59 (t, 2H, *J* = 7.6 Hz), 2.54 (t, 2H, *J* = 7.3 Hz), 1.80-1.91 (m, 7H), 1.61-1.78 (m, 6H), 1.36-1.51 (m, 4H), 0.96 (m, 42H), 0.68-0.74 (m, 2H), 0.60 (m, 14H). $^{13}$C NMR ($CDCl_3$): $\delta$ 172.4, 158.0, 144.5, 144.4, 141.1, 140.4, 136.4, 131.8, 131.8, 131.7, 128.1, 128.0, 126.7, 126.6, 114.0, 68.0, 65.1, 35.4, 35.3, 32.3, 31.8, 30.6, 30.1, 29.6, 29.0, 27.2, 26.2, 26.1, 26.0, 24.3, 24.2, 23.4, 22.9, 22.8, 12.0. $^{29}$Si NMR ($CDCl_3$): $\delta$ -59.0. IR (thin film): *v* = 3054, 3025, 2954, 2930, 2869, 1739, 1606, 1508, 1493, 1466, 1444, 1402, 1384, 1367, 1333, 1231, 1107, 839, 762, 745, 699 $cm^{-1}$. MALDI-TOF: [M] calcd for $C_{66}H_{104}O_{14}SSi_8$, m/z 1376.53; found, m/z 1376.69. Anal. Calcd for $C_{66}H_{104}O_{14}SSi_8$: C, 57.51; H, 7.61; S, 2.33; Si, 16.30. Found: C, 57.39; H, 7.70; S, 2.31; Si, 16.22.

**POSS-AN$_{21}$**. Yield = (59.1%). $^1$H NMR ($CDCl_3$): $\delta$ 6.99-7.14 (m, 15), 6.91 (d, 2H, *J* = 8.9 Hz), 6.62 (d, 2H, *J* = 8.8 Hz), 4.08 (m, 2H), 3.86 (m, 2H), 2.76 (t, 2H, *J* = 7.5 Hz), 2.59 (t, 2H, *J* = 7.5 Hz), 2.54 (t, 2H, *J* = 7.4 Hz), 1.79-1.91 (m, 7H), 1.58-1.76 (m, 4H), 1.24-1.45 (m, 18H), 0.95 (m, 42H), 0.68-0.74 (m, 2H), 0.60 (m, 14H). $^{13}$C NMR ($CDCl_3$): $\delta$ 158.1, 144.5, 144.4, 132.9, 131.8, 131.7, 128.1, 128.0, 126.7, 126.6, 114.0, 68.2, 65.3, 35.4, 31.8, 30.1, 30.0, 29.9, 29.8, 29.7, 29.6, 29.0, 27.2, 26.5, 26.3, 26.1, 24.3, 24.2, 23.4, 22.9, 22.9, 12.0. $^{29}$Si NMR ($CDCl_3$): $\delta$ -59.0. IR (thin film): *v* = 3054, 3025, 2954, 2926, 1739, 1607, 1508, 1466, 1367, 1333, 1231, 1109, 839, 745, 699 $cm^{-1}$. MALDI-TOF: [M] calcd for $C_{72}H_{116}O_{14}SSi_8$, m/z 1460.62; found, m/z 1460.99. Anal. Calcd for $C_{72}H_{116}O_{14}SSi_8$: C, 59.13; H, 7.99; S, 2.19; Si, 15.36. Found: C, 59.05; H, 8.08; S, 2.14; Si, 15.29.

**Table S1** Optimization of thiol-ene click reaction.

| Entry | Solvent[a] | Catalyst[b] | Separated yield (%) | | |
|---|---|---|---|---|---|
| | | | POSS-$AN_8$ | POSS-$AN_{15}$ | POSS-$AN_{21}$ |
| 1 | THF | $Et_3N$ | 13.9 | | |
| 2 | THF | $PPh_3$ | 38.9 | | |
| 3 | THF | DABCO | 41.4 | | |
| 3 | DMF | DABCO | 20.6 | | |
| 4 | DMSO | DABCO | 22.9 | | |
| 5 | DMF/THF | DABCO | 44.3 | | |
| 6 | DMF/THF | DABCO | 48.0 | 43.8 | 44.9 |
| 7 | DMSO/THF | DABCO[c] | 56.2 | 54.1 | 55.3 |
| 8 | DMSO/THF | DABCO | 61.2 | 58.4 | 59.1 |
| 9 | DMSO/THF | $Et_3N$ | 19.9 | | |
| 10 | DMSO/THF | $PPh_3$ | 25.8 | | |

[a]The mix solvent is in volume ratio of 1:1. [b]The catalyst is 0.1 mol equivalent, temperature is 80 °C, [c]temperature is 70 °C.

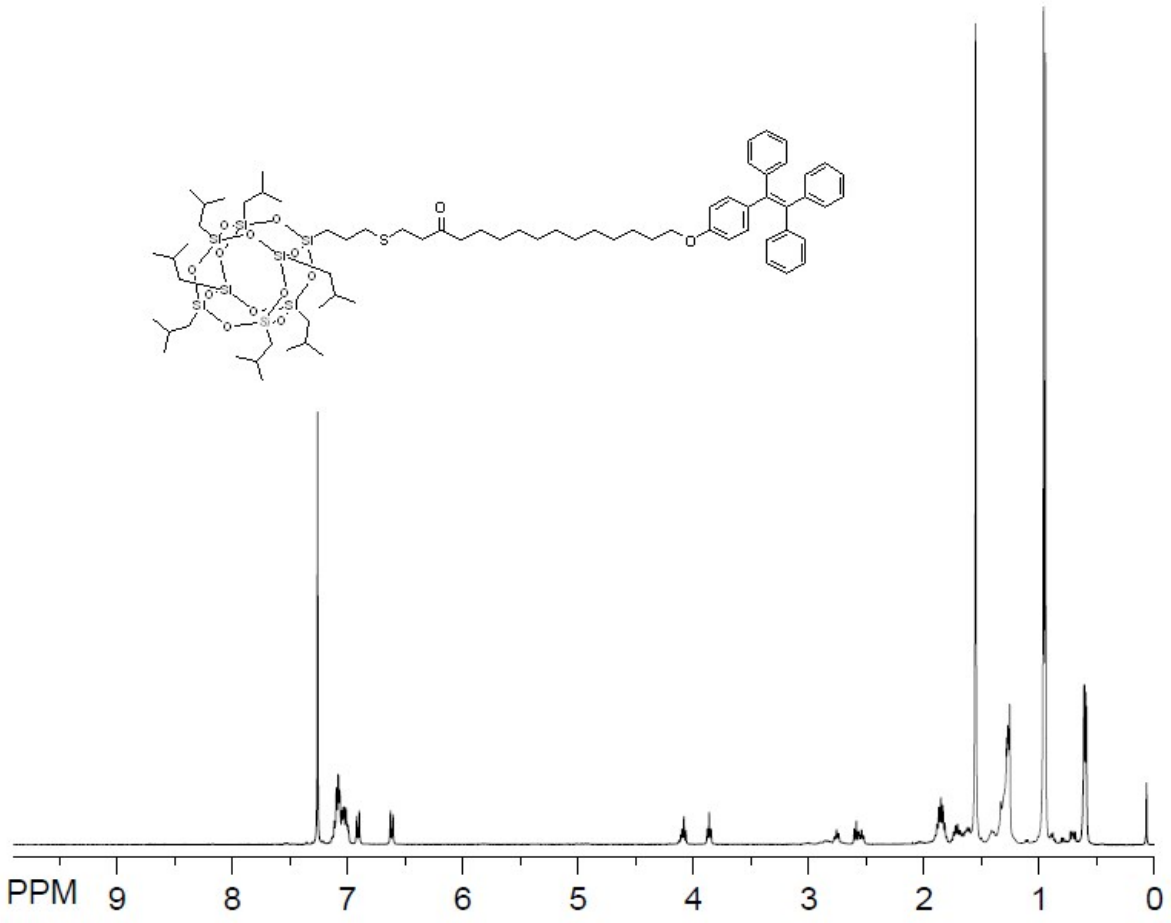


**Fig. S1** $^{1}H$ NMR of POSS-$AN_{21}$ in $CDCl_3$.

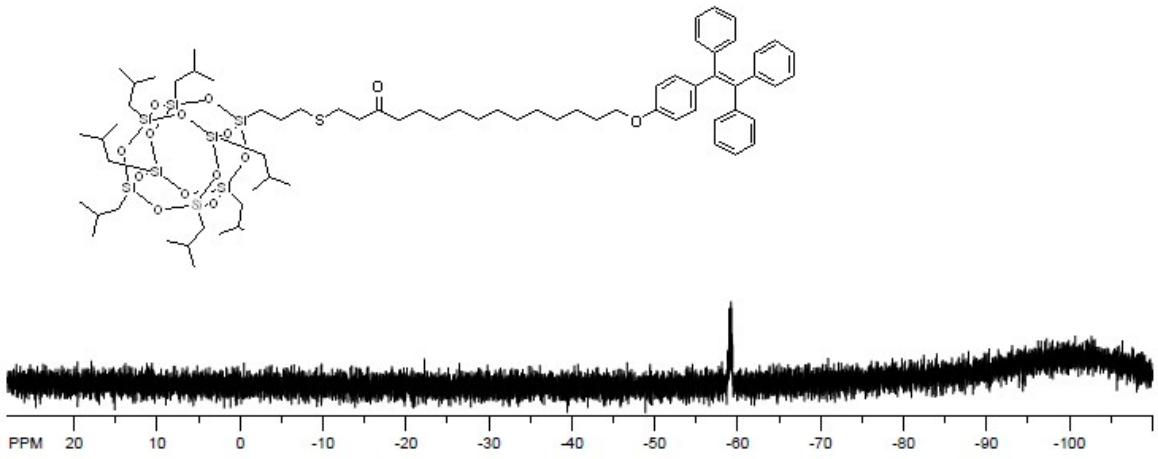


**Fig. S2** $^{29}Si$ NMR of POSS-$AN_{21}$ in $CDCl_3$.

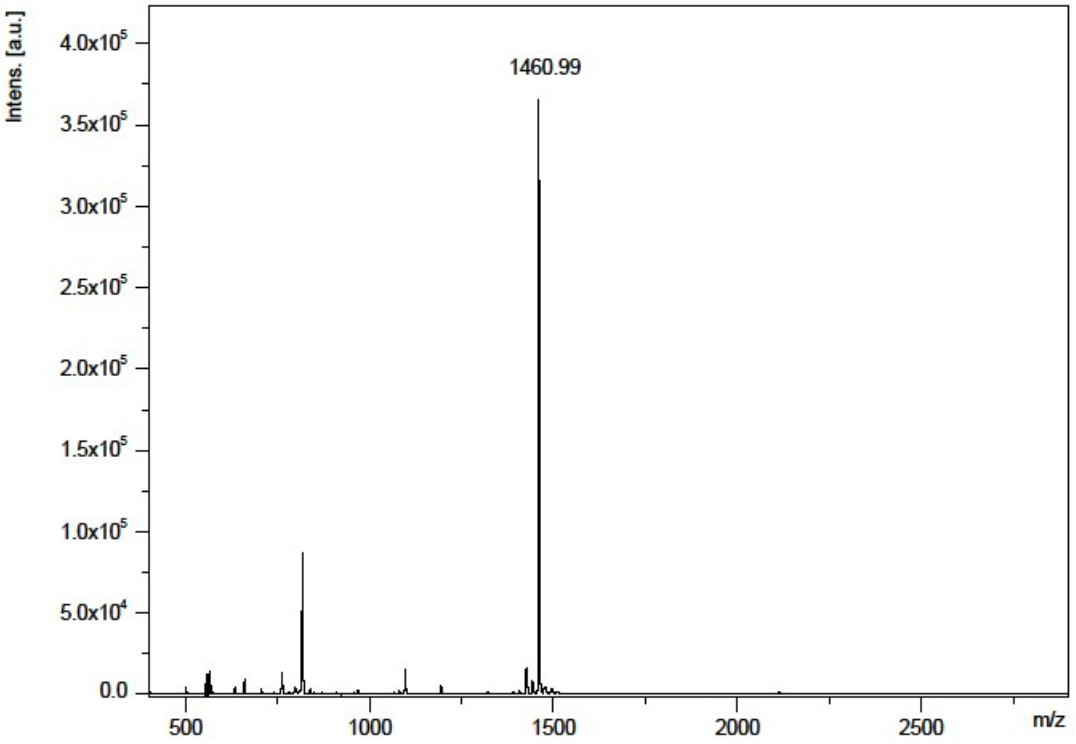


**Fig. S3** MALDI-TOF spectrum of POSS-$AN_{21}$.

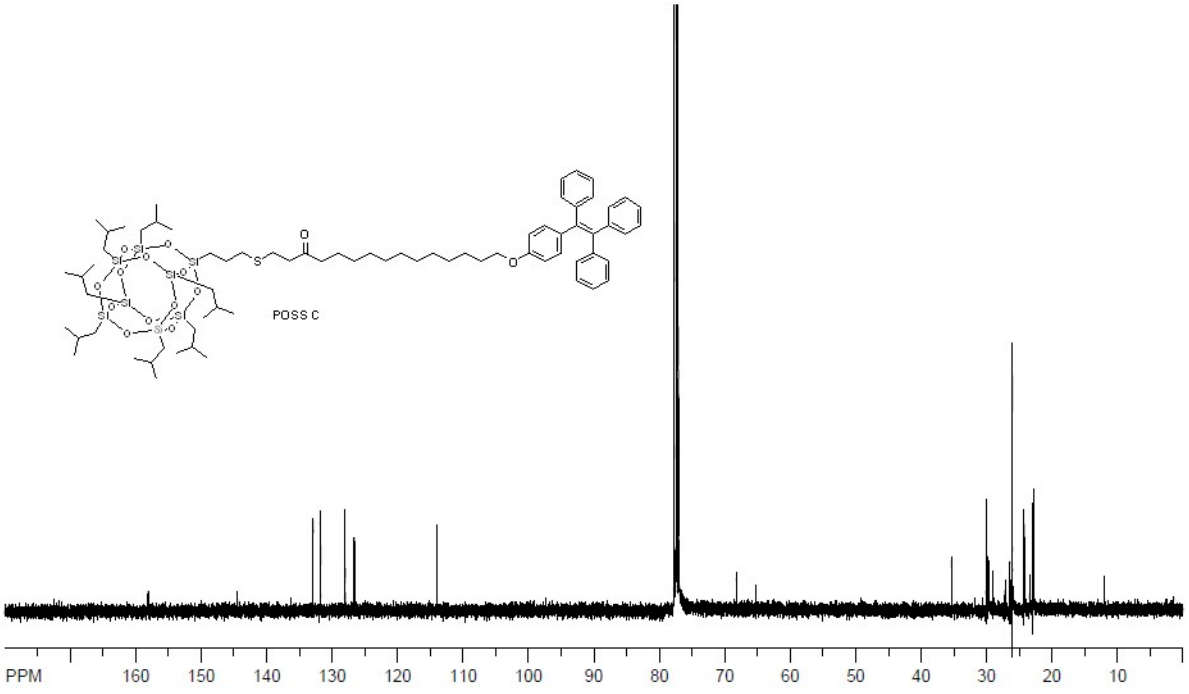


**Fig. S4** $^{13}C$ NMR of POSS-$AN_{21}$ in $CDCl_3$.

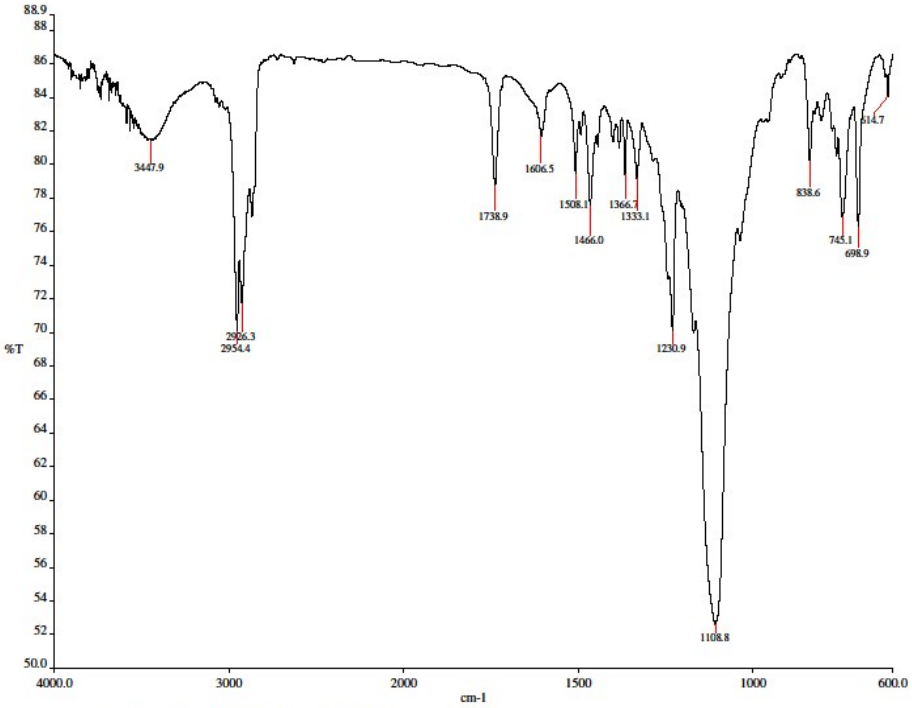


**Fig. S5** FTIR of POSS-$AN_{21}$ in KBr.

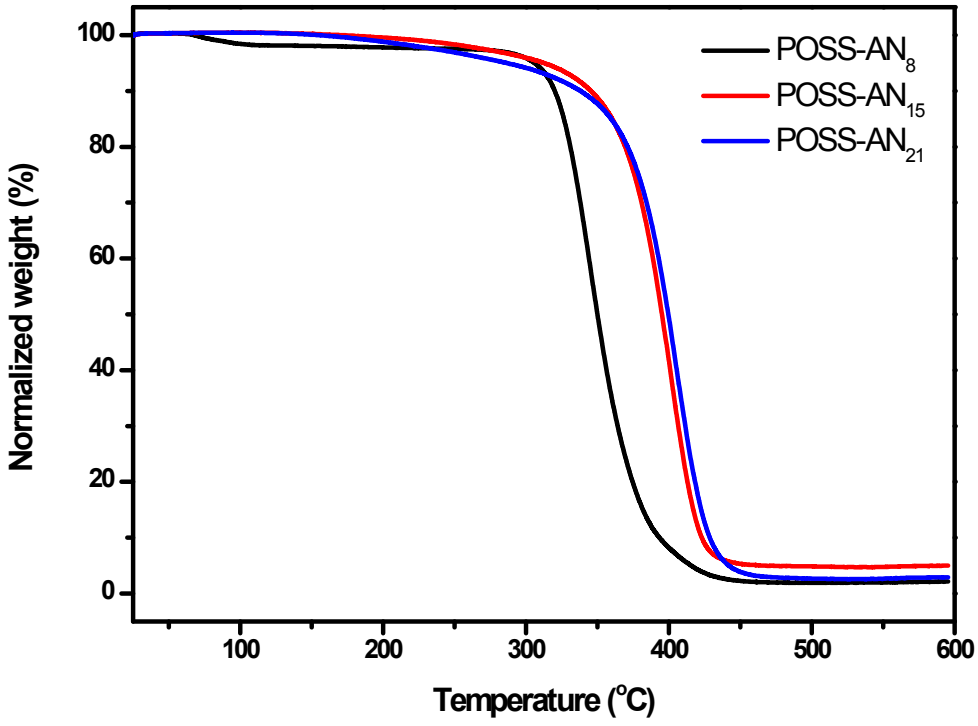


**Fig. S6** TGA thermograms of POSS-$AN_8$, POSS-$AN_{15}$ and POSS-$AN_{21}$ recorded under nitrogen at a heating rate of 20 °C/min.

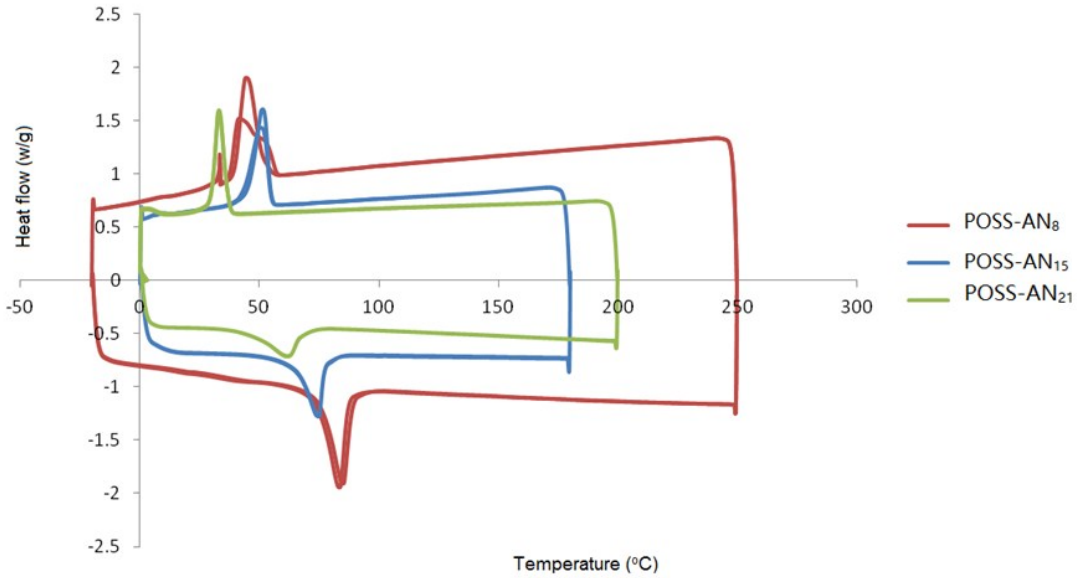


**Fig. S7** DSC thermograms of POSS-$AN_8$, POSS-$AN_{15}$ and POSS-$AN_{21}$ recorded under nitrogen at a heating rate of 10 °C/min.

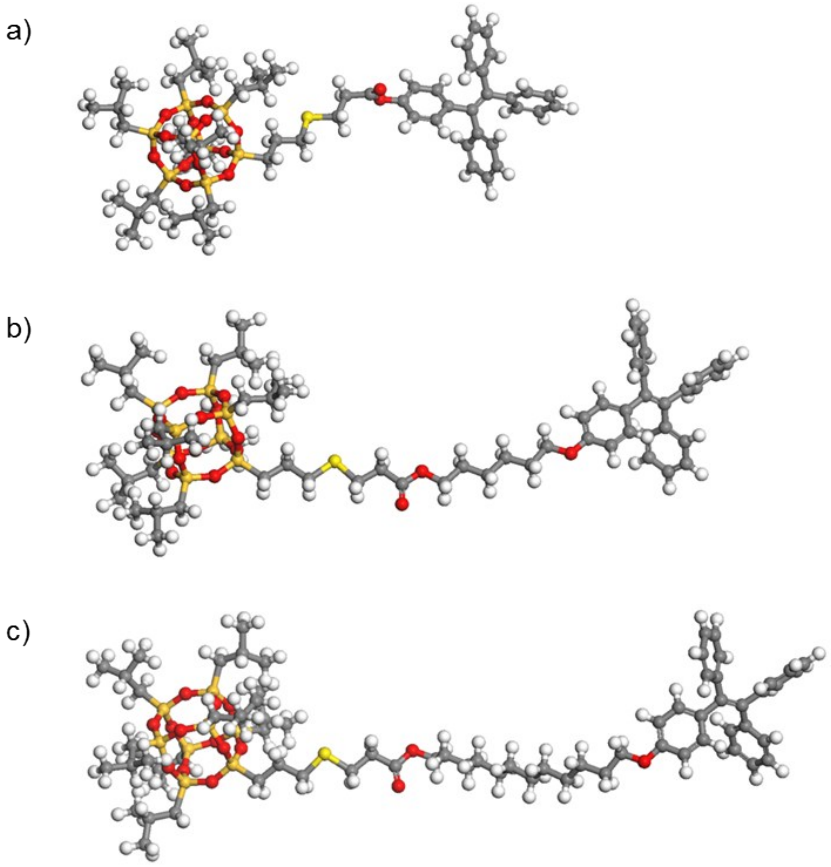


**Fig. S8** Optimized molecular structures of POSS-$AN_8$, POSS-$AN_{15}$ and POSS-$AN_{21}$ calculated using the B3LYP/6-31G(d,p) basis set.

**Table S2**. The surface area and occupied volume of POSS-$AN_8$, POSS-$AN_{15}$ and POSS-$AN_{21}$ calculated using the B3LYP/6-31G(d,p) basis set.

| Unit | d (Å) | Surface area ($Å^2$) | Occupied volume ($Å^3$) |
|---|---|---|---|
| POSS-$AN_8$ | 29.6 | 1210.6 | 1363.0 |
| POSS-$AN_{15}$ | 36.4 | 1321.1 | 1500.3 |
| POSS-$AN_{21}$ | 42.4 | 1421.6 | 1625.0 |

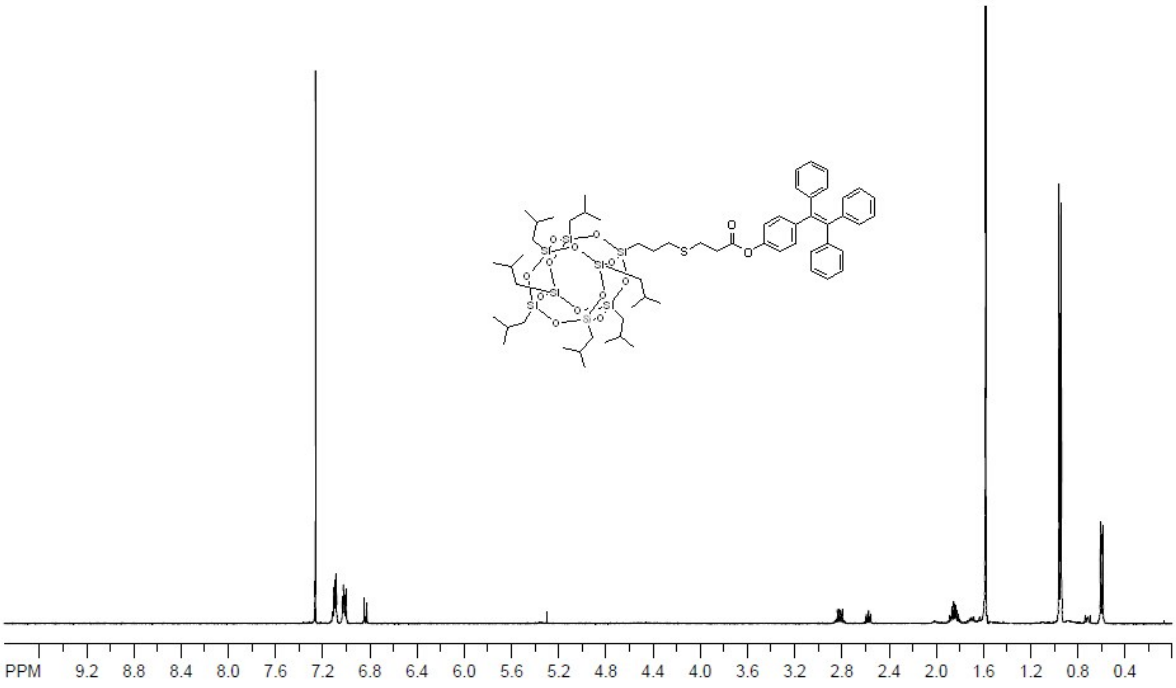


**Fig. S9** $^1H$ NMR of POSS-$AN_8$ in $CDCl_3$.

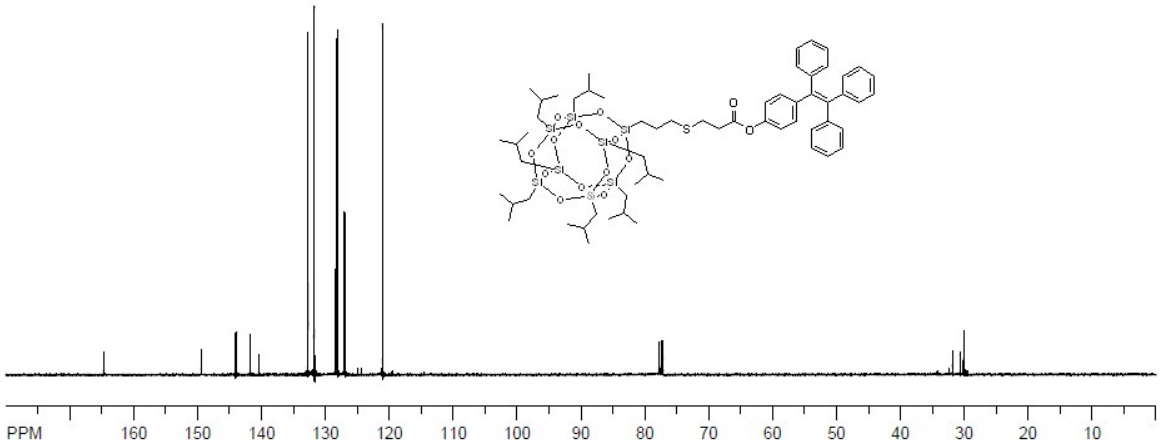


**Fig. S10** $^{13}C$ NMR of POSS-$AN_8$ in $CDCl_3$.

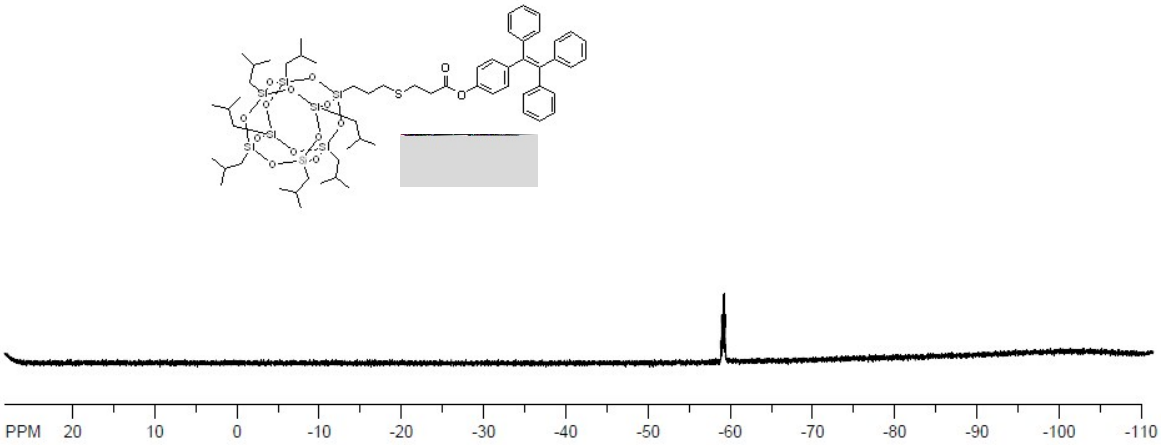


**Fig. S11** $^{29}Si$ NMR of POSS-$AN_8$ in $CDCl_3$.

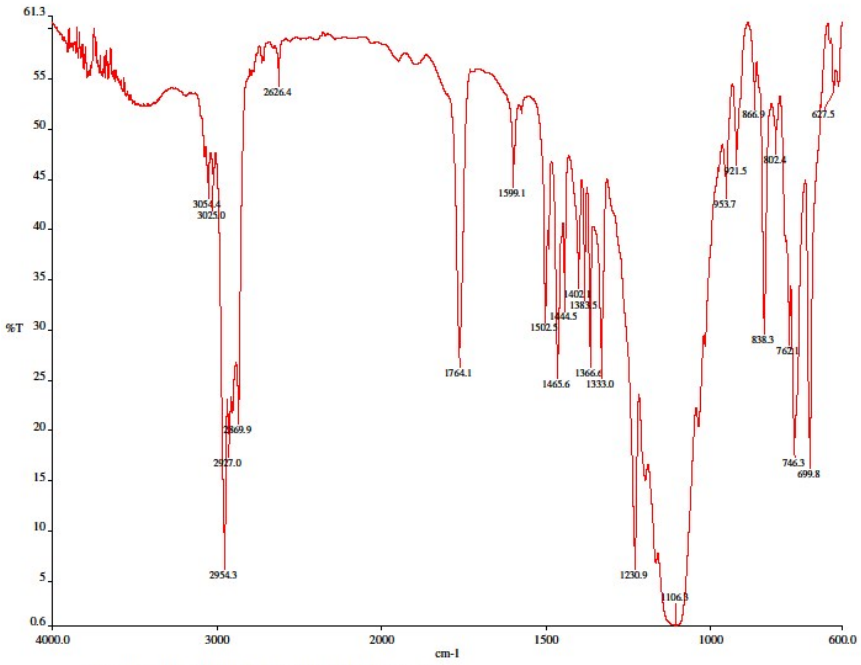


**Fig. S12** FTIR of POSS-$AN_8$ in KBr.

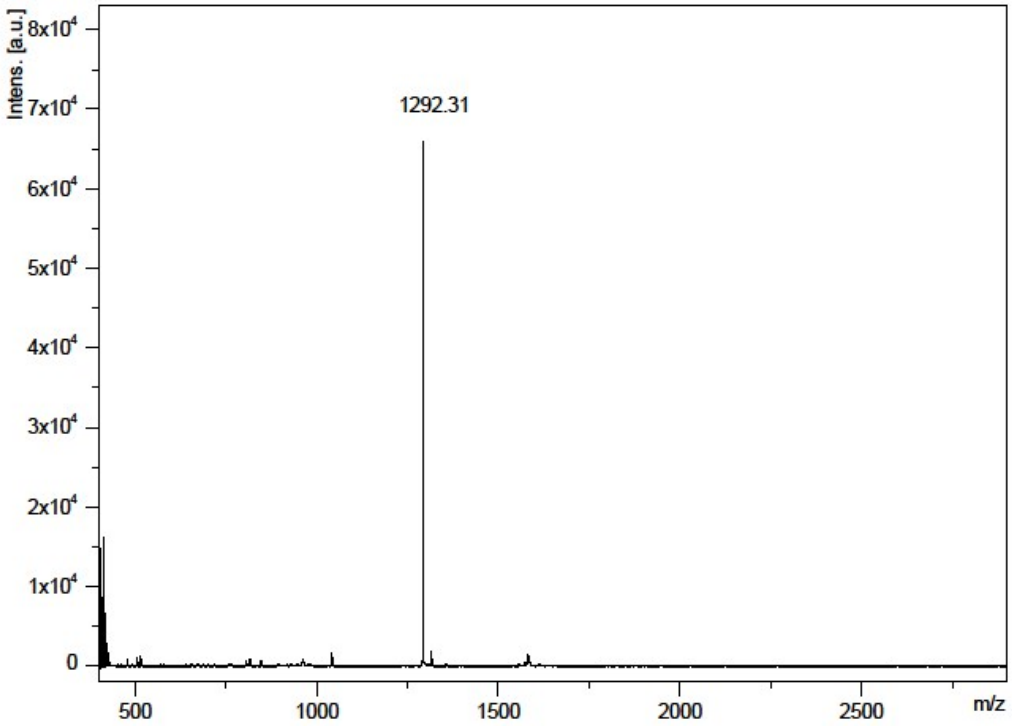


**Fig. S13** MALDI-TOF spectrum of POSS-$AN_8$.

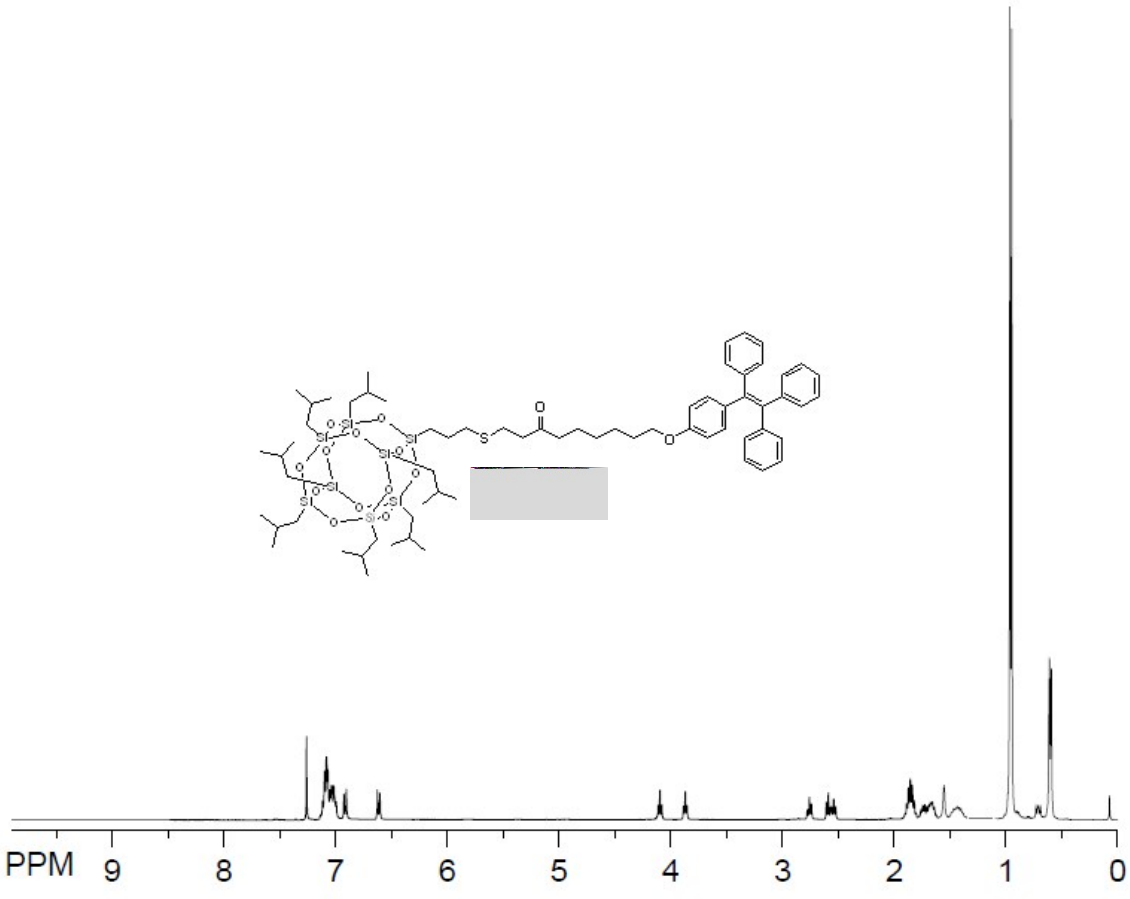


**Fig. S14** $^1H$ NMR of POSS-$AN_{15}$ in $CDCl_3$.

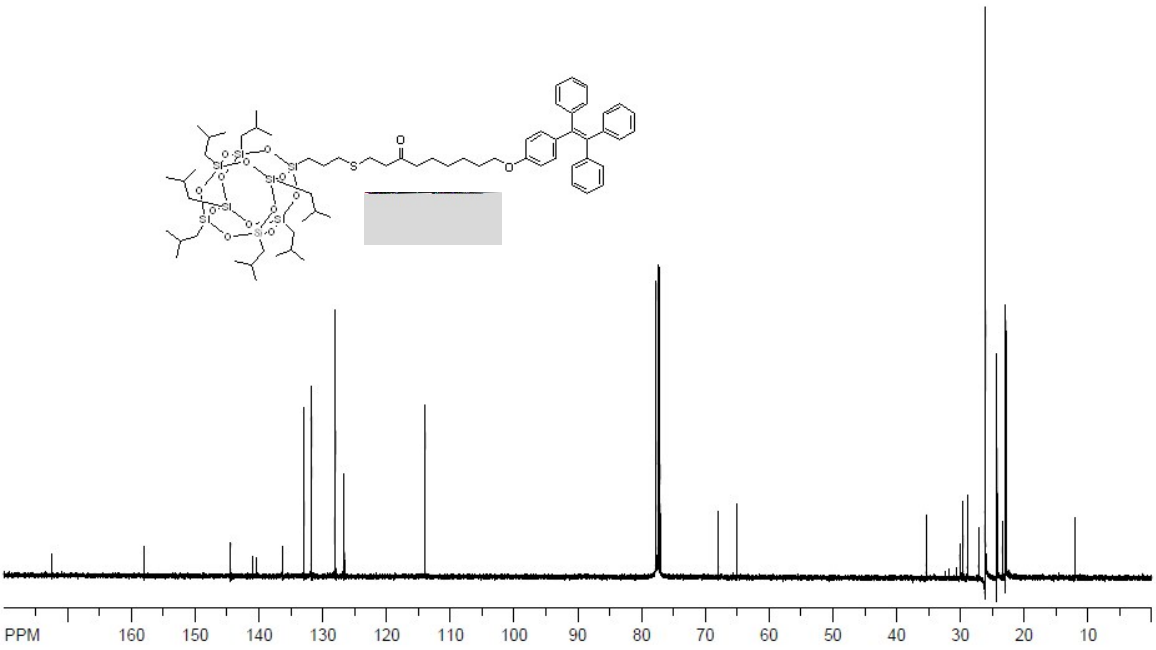


**Fig. S15** $^{13}C$ NMR of POSS-$AN_{15}$ in $CDCl_3$.

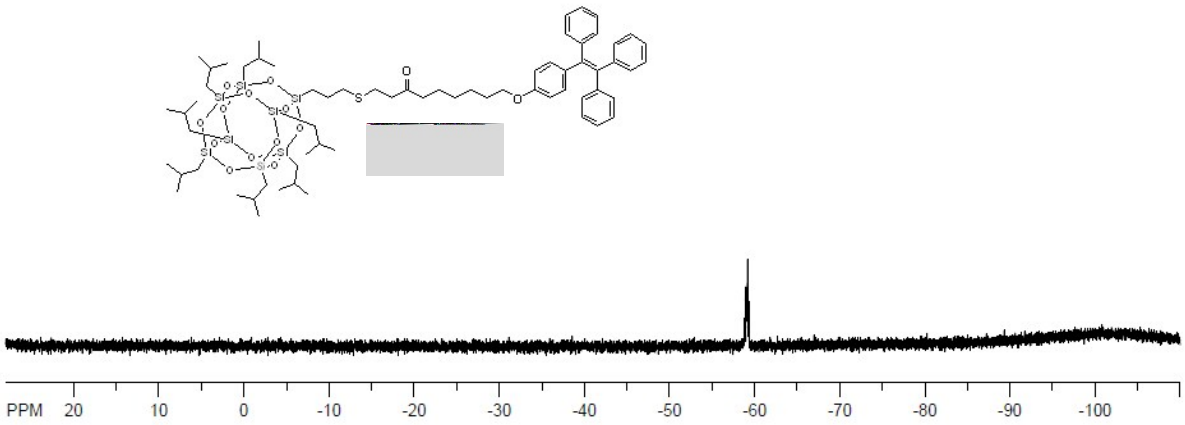


**Fig. S16** $^{29}Si$ NMR of POSS-$AN_{15}$ in $CDCl_3$.

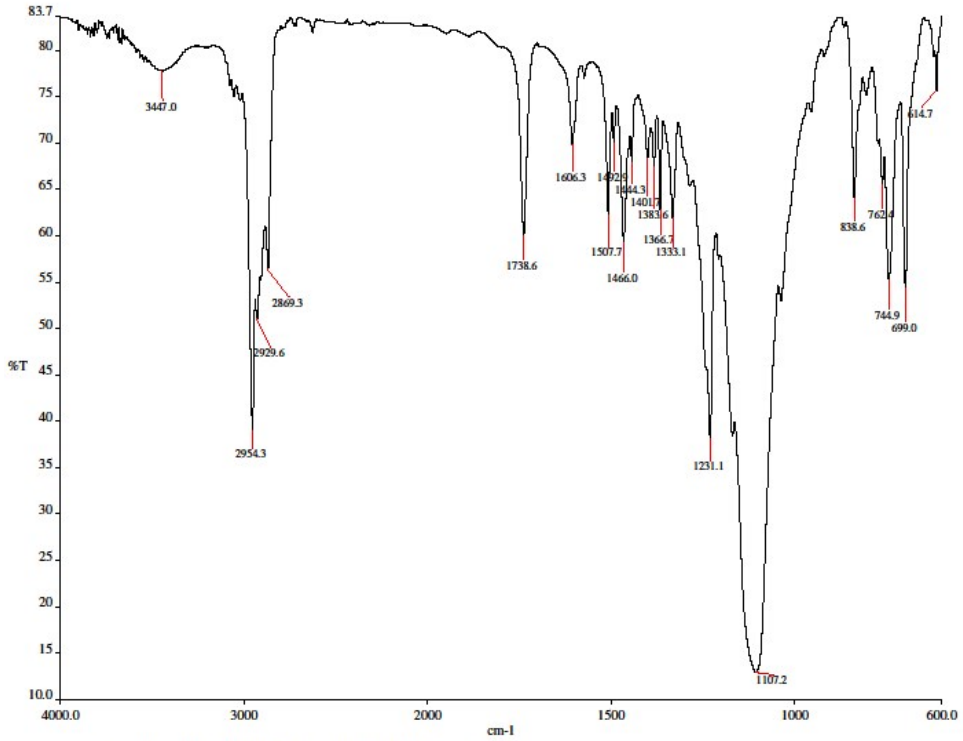


**Fig. S17** FTIR of POSS-$AN_{15}$ in KBr.

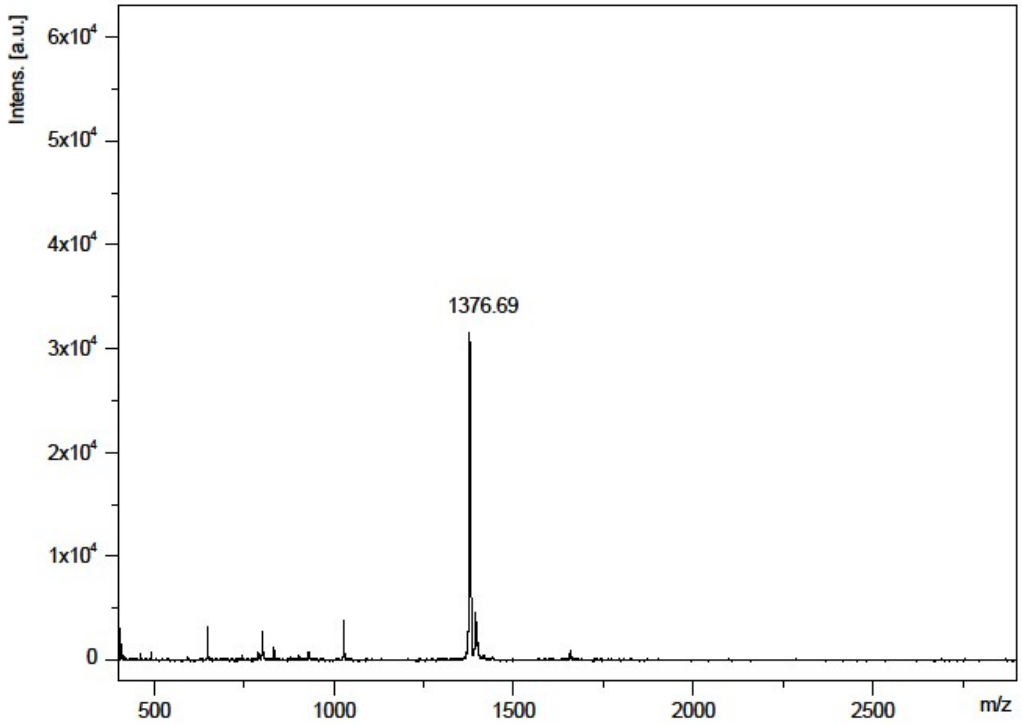


**Fig. S18** MALDI-TOF spectrum of POSS-$AN_{15}$.

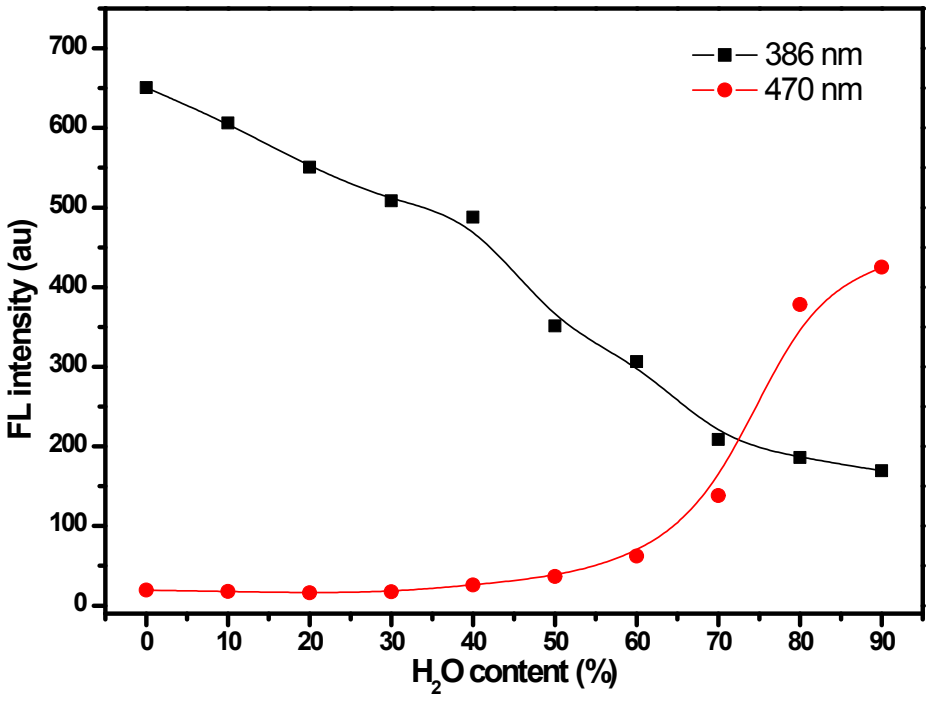


**Fig. S19** The curves of fluorescence intensity *vs* content of water measured of POSS-$AN_{21}$ at 386 nm (■) and 470 nm (●).

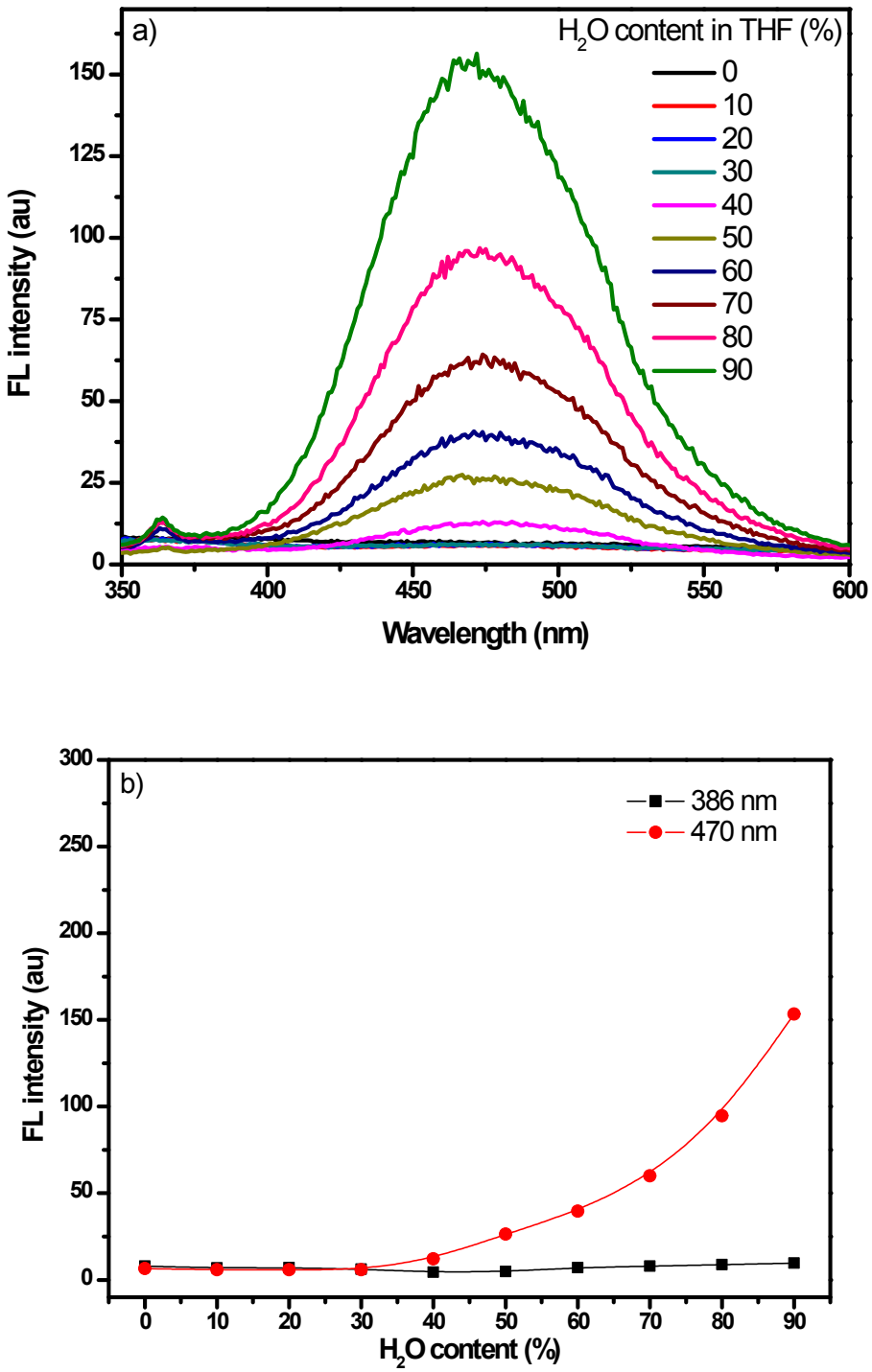


**Fig. S20** (a) Fluorescence spectra of POSS-$AN_8$ in THF/$H_2O$. $\lambda_{ex}$ = 318 nm, [C] = $10^{-4}$ M. (b) The curves of fluorescence intensity *vs* content of water measured of POSS-$AN_8$ at 386 nm (■) and 470 nm (●).

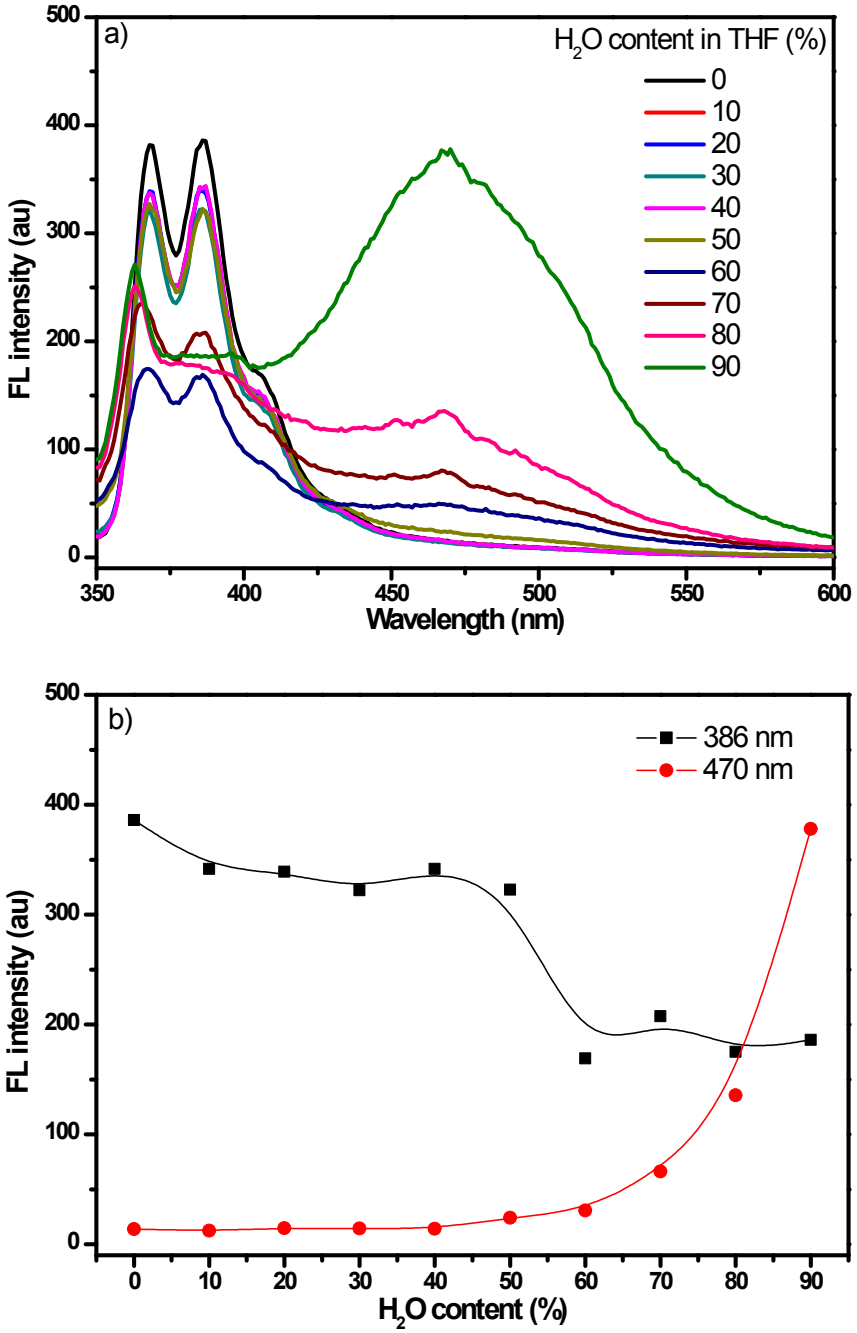


**Fig. S21** (a) Fluorescence spectra of POSS-AN$_{15}$ in THF/$H_2O$. $\lambda_{ex}$ = 318 nm, [C] = $10^{-4}$ M. (b) The curves of fluorescence intensity *vs* content of water measured of POSS-AN$_{15}$ at 386 nm (■) and 470 nm (●).

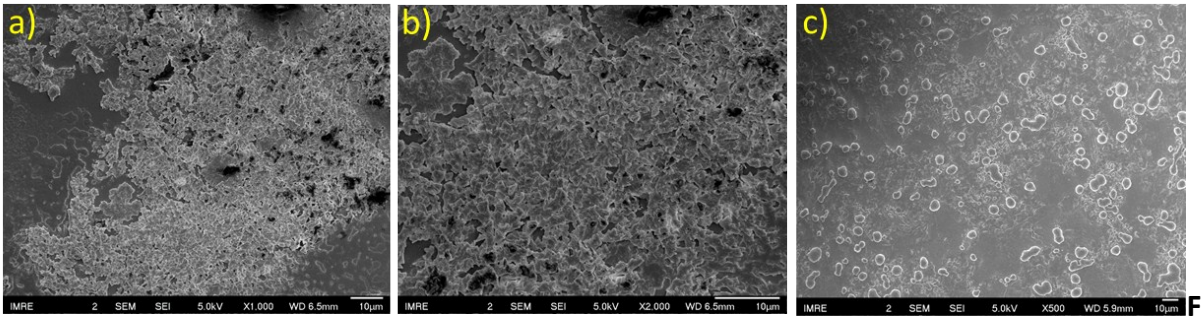


**Fig. S22** SEM images of solid samples prepared through air-drying the collected solution from column chromatography (hexane/dichloromethane): (a) POSS-$AN_8$, (b) POSS-$AN_{15}$ and (c) POSS-$AN_{21}$.

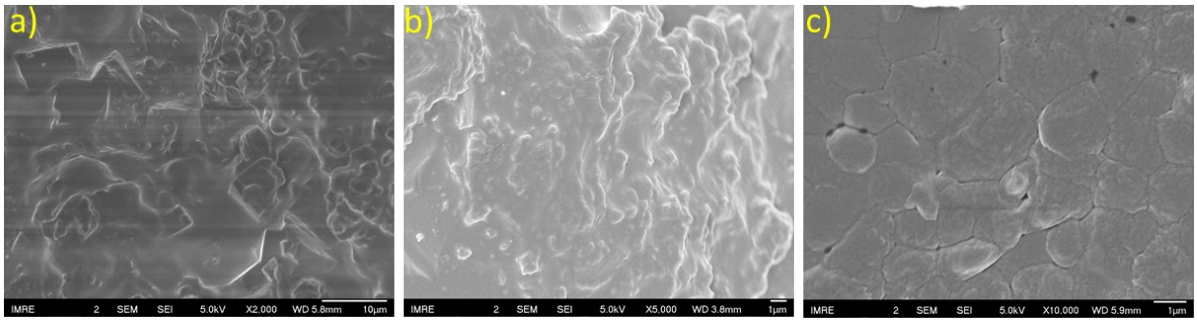


**Fig. S23** SEM images of solid samples prepared from THF solution by freeze drying to move THF: (a) POSS-$AN_8$, (b) POSS-$AN_{15}$ and (c) POSS-$AN_{21}$.

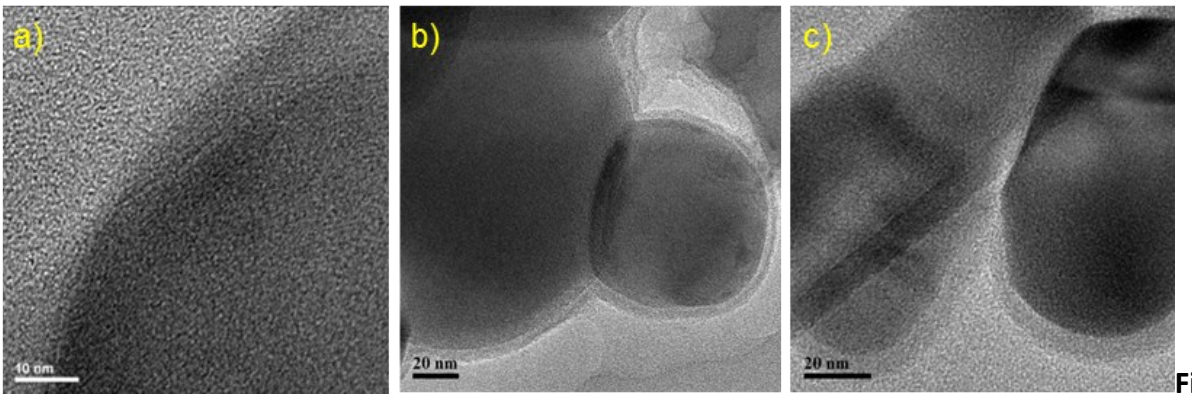


**Fig. S24** TEM images of solid samples prepared through air-drying the collected solution from column chromatography (hexane/dichloromethane): (a) POSS-$AN_8$, (b) POSS-$AN_{15}$ and (c) POSS-$AN_{21}$.

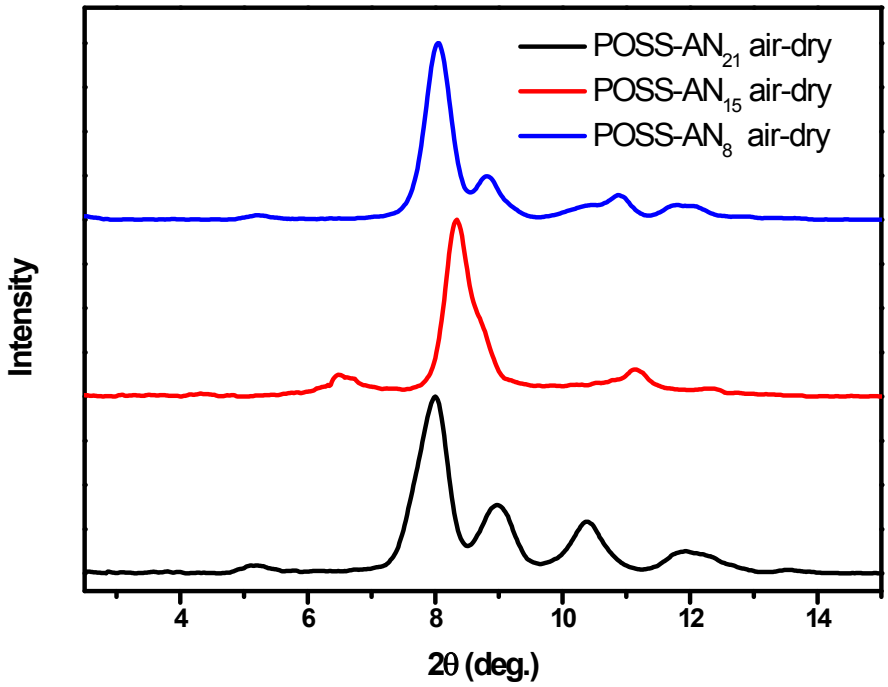


**Fig. S25** X-ray diffraction patterns at the low angle region of POSS-$AN_8$, POSS-$AN_{15}$ and POSS-$AN_{21}$. All samples are prepared through air-drying the collected solution from column chromatography (hexane/dichloromethane).

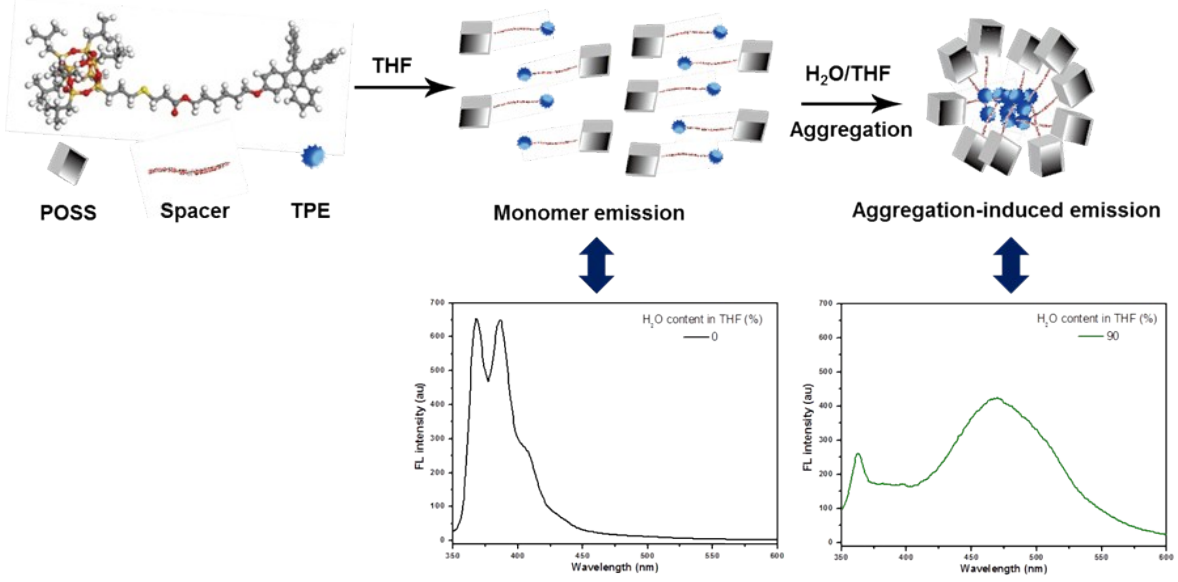


**Fig. S26** Illustration of self-assembly of TPE-modified POSS molecules in THF and THF/water.